Water Resources Research

RESEARCH ARTICLE
10.1029/2023WR035721

Leveraging ICESat, ICESat-2, and Landsat for Global-Scale, Multi-Decadal Reconstruction of Lake Water Levels

Fangfang Yao[1,2], Ben Livneh[1,3], Balaji Rajagopalan[1,3], Jida Wang[4,5], Kehan Yang[6,7], Jean-François Crétaux[8], Chao Wang[9], and J. Toby Minear[1]

[1]Cooperative Institute for Research in Environmental Sciences (CIRES), University of Colorado Boulder, Boulder, CO, USA, [2]Environmental Institute (EI), University of Virginia, Charlottesville, VA, USA, [3]Department of Civil, Environmental and Architectural Engineering, University of Colorado Boulder, Boulder, CO, USA, [4]Department of Geography and Geographic Information Science, University of Illinois Urbana-Champaign, Urbana, IL, USA, [5]Department of Geography and Geospatial Sciences, Kansas State University, Manhattan, KS, USA, [6]Department of Civil & Environmental Engineering, University of Washington, Seattle, WA, USA, [7]eScience Institute, University of Washington, Seattle, WA, USA, [8]Laboratoire d'Études en Géophysique et Océanographie Spatiales (LEGOS), CNES-IRD-CNRS-UT3, Centre National d'Études Spatiales (CNES), Université de Toulouse, Toulouse, France, [9]Department of Earth, Marine and Environmental Sciences, University of North Carolina, Chapel Hill, NC, USA

Abstract Lakes provide important water resources and many essential ecosystem services. Some of Earth's largest lakes recently reached record-low levels, suggesting increasing threats from climate change and anthropogenic activities. Yet, continuous monitoring of lake levels is challenging at a global scale due to the sparse in situ gauging network and the limited spatial or temporal coverage of satellite altimeters. A few pioneering studies used water areas and hypsometric curves to reconstruct water levels but suffered from large uncertainties due to the lack of high-quality hypsometry data. Here, we propose a novel proxy-based method to reconstruct multi-decadal water levels from 1992 to 2018 for both large and small lakes using Landsat images and ICESat (2003–2009) and recently launched ICESat-2 (2018+) laser altimeters. Using the new method, we evaluate reconstructed levels of 342 lakes worldwide, with sizes ranging from 1 to 81,844 km^2. Reconstructed water levels have a median root-mean-square error (RMSE) of 0.66 m, equivalent to 57% of the standard deviation of monthly level variability. Compared with two recently reconstructed water level data sets, the proposed method reduces the median RMSE by 27%–32%. The improvement is attributable to the new method's robust construction of high-quality hypsometry, with a median R^2 value of 0.92. Most reconstructed water level time series have a bi-monthly or higher frequency. Given that ICESat-2 and Landsat can observe hundreds of thousands of water bodies, this method can be applied to conduct an improved global inventory of time-varying lake levels and thus inform water resource management more broadly than existing methods.

Key Points:

- Landsat images and laser altimeters were leveraged to reconstruct multi-decadal lake levels of both large and small lakes
- Reconstructed water levels were validated against observed levels on 342 global lakes with a median error of 0.66 m
- Most of the reconstructed lake level time series have a bi-monthly or higher frequency

Supporting Information:

Supporting Information may be found in the online version of this article.

Correspondence to:

F. Yao,
fangfang.yao@colorado.edu;
yaoff.luke@gmail.com

Citation:

Yao, F., Livneh, B., Rajagopalan, B., Wang, J., Yang, K., Crétaux, J.-F., et al. (2024). Leveraging ICESat, ICESat-2, and Landsat for global-scale, multi-decadal reconstruction of lake water levels. *Water Resources Research*, *60*, e2023WR035721. https://doi.org/10.1029/2023WR035721

Received 27 JULY 2023
Accepted 27 JAN 2024

Author Contributions:

Conceptualization: Fangfang Yao
Formal analysis: Fangfang Yao
Funding acquisition: Fangfang Yao
Methodology: Fangfang Yao, Balaji Rajagopalan, Kehan Yang, Chao Wang
Validation: Fangfang Yao, Jean-François Crétaux
Visualization: Fangfang Yao, Ben Livneh, Jida Wang, Kehan Yang
Writing – original draft: Fangfang Yao

1. Introduction

Lakes, including natural lakes and human-regulated reservoirs, provide many essential ecosystem services, ranging from water and food supply (Alsdorf et al., 2007; McIntyre et al., 2016), wildlife habitats (Wurtsbaugh et al., 2017), cycling of pollutants and nutrients (Bastviken et al., 2011; Williamson et al., 2009), to recreational opportunities like boating, fishing, and landscape aesthetics. The ecological and sociological functions of lakes are largely modulated by water levels (Wurtsbaugh et al., 2017). Changes in precipitation, river inflow, evaporation, or a combination thereof can lead to major shifts in lake level (Chen et al., 2017). Human activities, such as damming, river diversion, and water withdrawal, can also impact lake levels (Al-Weshah, 2000; Chaudhari et al., 2018; Crétaux et al., 2013; Micklin, 1988; J. Wang et al., 2013, 2017, 2018; Wurtsbaugh et al., 2017). Some of Earth's largest lakes, such as Lakes Mead and Michigan-Huron in the United States, and the Aral Sea in Central Asia, recently reached record-low levels, suggesting increasing threats from climate change and human activities (Barnett & Pierce, 2008; Crétaux et al., 2013; Gronewold & Stow, 2014; J. Wang et al., 2018; Wurtsbaugh et al., 2017; Yao et al., 2023). The water level declines of large lakes have widespread impacts including water scarcity, crop failure, environmental degradation, and hydropower energy reduction (Tilzer & Serruya, 1990). Alternatively, warming-induced increases in runoff from glacier retreat can partially contribute to rising lake levels, such as in the Tibetan Plateau, indicating increased vulnerability of high mountain residents to glacial lake outburst floods (Shugar et al., 2020; Yao et al., 2018). Therefore, accurate knowledge of lake level variability is

Writing – review & editing: Fangfang Yao, Ben Livneh, Balaji Rajagopalan, Jida Wang, Kehan Yang, Jean-François Crétaux, Chao Wang, J. Toby Minear

critical for assessing changes in freshwater availability and water-related hazards, and for sustainable water resource management to support the needs of both humans and the environment.

Despite its critical importance, continuous monitoring of lake levels is rare at the global scale due to observational challenges (Crétaux et al., 2011). In situ measurements are spatially sparse and are in decline (Schwatke et al., 2015). Satellite remote sensing provides a promising alternative for measuring lake level changes. Since the 1990s, radar altimetry has been used to measure inland water levels at sub-monthly to monthly intervals (Crétaux et al., 2011). These radar altimeters provide level measurements with decimeter accuracy for large lakes (Gao et al., 2012; X. Li et al., 2019). Several databases, including Hydroweb (Crétaux et al., 2011), the Global Reservoir and Lake Monitor (G-REALM) (Birkett et al., 2011), and the Database for Hydrological Time Series of Inland Waters (DAHITI) (Schwatke et al., 2015), provide time-varying lake levels at sub-monthly to monthly intervals. However, owing to the coarse footprints of the radar altimeters (typically 10 km or so) and large inter-track distance (>70 km), only a few hundred of the world's largest water bodies are continuously observed by satellite radar altimeters for more than one decade over the past 30 years (Cooley et al., 2021).

Recent advances in laser altimeters have enabled more extensive monitoring of lake levels because of their smaller footprints (e.g., ≤70 m) (Cooley et al., 2021; Ma et al., 2024; Madson & Sheng, 2021; Y. Wang et al., 2023; Yuan et al., 2020; Zhang et al., 2011). The Ice, Cloud, and land Elevation Satellite (ICESat) provides water level measurements for thousands of inland water bodies with an accuracy of a few centimeters from 2003 to 2009 at a 91-day interval (Schutz et al., 2005). To continue the legacy, its successor ICESat-2 was launched in 2018. Owing to improved accuracy and spatial resolution, ICESat-2 data were leveraged to estimate variations in water levels during 2018–2020 for 227,386 water bodies worldwide (Cooley et al., 2021). More recently, Luo et al. (2022) combined ICESat and ICESat-2 to estimate level variations for 6,567 lakes from 2003 to 2020. However, their derived level time series suffers from a 9-year discontinuity due to the gap between ICESat and ICESat-2 missions. Therefore, these existing attempts that directly rely on water levels from laser altimeters do not provide continuous monitoring of lake levels for periods longer than 8 years.

Lake water levels also can be estimated indirectly via proxy approaches where lake area serves as a proxy for water level. In contrast with water levels, lake areas are easier to observe via satellites. Satellite-derived lake areas show strong correlations with water levels (Crétaux et al., 2016; Gao et al., 2012; Yao et al., 2019). Using the series of Landsat satellites (Landsat 4, 5, 7, and 8), lake water areas can be constructed from the 1980s (or 1990s depending on geographic locations) to the present at a 30-m resolution. Due to a relatively coarse temporal resolution (16 days) and cloud contamination, high-frequency reconstruction of long-term lake areas has been impeded until very recently. To increase the temporal frequency of lake area time series, advanced algorithms have been developed to estimate lake areas from partially contaminated images (L. Feng et al., 2023; Schwatke et al., 2019; Yao et al., 2019; Zhao & Gao, 2018). For example, Yao et al. (2019) constructed a high-frequency long-term lake area data set Global Lake/Reservoir Area Time Series (GLATS) by leveraging both good-quality and contaminated Landsat images. However, water areas alone do not provide direct information on water level that is critical for various applications in hydrology (Cooley et al., 2021; Tokuda et al., 2021; Yao et al., 2018), water resources management (Dawadi & Ahmad, 2012; Rosenberg, 2022), limnology (Bootsma & Hecky, 1993; Hipsey et al., 2019), and ecological conservation (Wurtsbaugh & Sima, 2022). In particular, lake level is often the most crucial variable that determines water storage variability (Cooley et al., 2021). Understanding lake water budgets relies significantly on this factor (Yao et al., 2018). Therefore, proxy approaches require a prior area-level relationship, referred to as lake hypsometry or a hypsometric curve, to convert lake areas to water levels.

Lake hypsometry can be constructed from lake bathymetry, although bathymetry data are sparse. ICESat and ICESat-2 provide new opportunities for deriving lake hypsometry owing to high-resolution laser measurements of Earth's surface elevation. These elevation measurements can be combined with lake contours (isobaths) to derive the hypsometry. Y. Li et al. (2020) used ICESat and radar altimetry in combination with the Global Surface Water (GSW) data set (Pekel et al., 2016) to construct lake hypsometry of 347 global reservoirs larger than 50 km^2. Given the higher resolution (17 m), smaller along-track spacing (0.7 m), and more laser beams of ICESat-2, it is now possible to construct lake hypsometry with improved accuracy and spatial coverage. Very recently, a few studies leveraged ICESat/ICESat-2 and Landsat to estimate lake volume changes in thousands of lakes worldwide at a decadal scale (Y. Feng et al., 2022; Y. Li et al., 2023; Luo et al., 2022; Yao et al., 2023). However, high-quality hypsometry is limited to a few hundred lakes (Crétaux et al., 2016; Y. Li et al., 2023; Yao et al., 2023). Thus, these pioneering studies often reconstructed water levels or volumes using simplified

Table 1
Summary of Existing Global-Scale Studies on Water Levels or Volumes at a Decadal Scale Using ICESat or ICESat-2 Altimetry

Study	Number of studied lakes	Number of lakes in validation	Validated variable	Hypsometry
Y. Feng et al. (2022)	9,065	14	Level; volume	Simplified hypsometry for 9,065 lakes
Y. Li et al. (2023)	7,245	277	Volume	Empirical models for 6,637 lakes and well-calibrated hypsometry for 347 lakes
Luo et al. (2022)	6,567	0	N/A	None
Yao et al. (2023)	1,972	102	Volume	Simplified hypsometry for 1,505 and well-calibrated hypsometry for 401 lakes

hypsometry or empirical methods (Table 1). For example, Y. Feng et al. (2022) combined ICESat, ICESat-2, and Landsat-derived water areas from the GSW data set to estimate time-varying water levels and volumes for 9,065 lakes globally over the period 2003–2020. They used water areas from the GSW and an overall area-level slope based on bootstrapping simulations to reconstruct water levels. However, the uncertainties of their reconstructed levels appear to be large probably due to the lack of high-quality hypsometry and the validation was limited to 14 lakes. This is particularly concerning given the large influence of hypsometry on the accuracy of estimated levels (Crétaux et al., 2016; Weekley & Li, 2021).

The overarching goal of this study is to develop and validate an improved proxy-based approach for reconstructing multi-decadal lake levels over the period 1992–2018 using water areas mapped from 30-m Landsat images and high-resolution laser altimeters ICESat-2 and ICESat. The method is described in detail in Section 3, but a quick overview is provided here. Using near coincident measurements of lake water level from laser elevation measurements (ICESat and ICESat-2) combined with water area observations from Landsat, we calculated a hypsometric function to define the area-level relationship. Then, the hypsometric function was used to convert the multi-decadal water area time series (1992–2018) in the GLATS database to water levels. We demonstrated the performance of this approach through validation of reconstructed water levels for 342 water bodies worldwide, with sizes ranging from 1 to 81,844 km^2, against observed long-term water levels from in situ gauges or radar altimeters. Given that Landsat and ICESat-2 can jointly observe hundreds of thousands of water bodies globally (Cooley et al., 2021; Khandelwal et al., 2022), the proposed method has the potential to improve the global inventory of time-varying lake levels and thus informs water resource management to a greater extent.

2. Data Sets

2.1. ICESat and ICESat-2

We used the ICESat L2 Global Land Surface Altimetry product (GLAH14) and the latest release (version 6) of the ICESat-2 L3A Land and Vegetation Height product (ATL08) for deriving water levels. ICESat provides laser pulses with a footprint of 70 m and an along-track sampling interval of 170 m at a 91-day repeat cycle (Abdalati et al., 2010). ICESat-2 has the same repeat period with a finer footprint (17 m) and a smaller along-track interval (0.7 m) (Markus et al., 2017). While ICESat has only one beam in the along-track direction, ICESat-2 has 6 beams, leading to higher accuracy and better spatial coverage (Abdalati et al., 2010; Markus et al., 2017). We utilized measurements of terrain height and water surface elevation from both the GLAH14 and ATL08 products. Specifically, the "d_elev" variable from GLAH14 and the "h_te_mean" variable from ATL08 were used. The accuracy of water levels derived from GLAH14 and ATL08 is reported to be approximately 0.38 and 0.14 m, respectively (Y. Feng et al., 2022; Ryan et al., 2020).

2.2. Landsat Images

To map water extents during the ICESat/ICESat-2 passes, the 30-m top-of-atmosphere images from Landsat 5 Thematic Mapper (TM), Landsat 7 Enhanced TM Plus (ETM+), Landsat 8 Operational Land Imager (OLI), and Landsat 9 OLI sensors, were used. We used top-of-atmosphere reflectance products rather than surface reflectance products, as suggested by existing studies on surface water extents (Allen & Pavelsky, 2018; Donchyts et al., 2016; Pekel et al., 2016; Sheng et al., 2016; Yao et al., 2019). To avoid cumbersome data storage, all used

Table 2
Summary of Reference Level Data Sets for Reconstructed Water Levels in Small and Large Lakes

Reference data sets	Number of included small lakes studied here	Number of included large lakes studied here	References
In situ measurements	48	80	N/A (see Data Availability Statement for data access)
Radar altimetry level products	0	214	Birkett et al. (2011), Crétaux et al. (2011), and Schwatke et al. (2015)
Total	48	294	

images were accessed and processed online from the cloud-based platform Google Earth Engine (Gorelick et al., 2017).

2.3. Global Surface Water Data Set

We used the water occurrence map in the GSW data set version 1.3 (Pekel et al., 2016) to generate water masks, similar to Cooley et al. (2021) (see Section 3.2.2 for more details). This water occurrence map was derived from all Landsat images from 1984 to 2020 at a 30-m resolution. In this map, water occurrence was calculated as the ratio of the total times of a pixel being classified as water to the total number of valid and non-contaminated observations, ranging from 0 (permanent land) to 100% (permanent water).

2.4. Global Lake and Reservoir Area Time Series Data Set

We collated multi-decadal water area records from the GLATS data set (Yao et al., 2019). The GLATS provides long-term high-frequency time series of global lake and reservoir areas over the period 1992–2018 using Landsat images, including both contamination-free and partially contaminated images. Owing to leveraging contaminated images to increase observation frequency, the temporal frequency of water area time series in the GLATS is generally higher than bi-monthly (once per 2 months) with the exception of lakes during a prolonged frozen season in high-latitude or high-altitude regions. The mean error of water areas is reported to be only 2.2%. The GLATS currently includes 576 water bodies worldwide.

2.5. Reference Water Levels

To validate the reconstructed water levels, this study used water levels observed from in situ gauging stations and radar altimeters. In situ level data were collected from multiple sources, such as the USGS National Water Information System and the Australian Bureau of Meteorology (see "Data Availability Statement" for details). When in situ level data were not available, we collected the radar-altimeter-derived water level products from three major databases, including Hydroweb (Crétaux et al., 2011), DAHITI (Schwatke et al., 2015), and G-REALM (Birkett et al., 2011). The overall accuracy of radar altimetry-derived water levels for inland water bodies ranges from a few centimeters for large water bodies to several decimeters for small and narrow water bodies. As the accuracy for small water bodies is relatively low, we discarded radar altimetry levels for small lakes, defined as water area less than 50 km^2 (Y. Li et al., 2020; Tao et al., 2015; Yao et al., 2018), and only used in situ levels for these smaller lakes instead (Table 2).

3. Methods

We identified 342 lakes for testing the performance of our proposed methodology (Section 3.1). This effort is geared toward devising a novel method and evaluating its performance at a global scale, rather than generating a detailed global data set for all water bodies observed by Landsat and ICESat-2. Our validation of the method on 342 global lakes is more extensive than most of the existing studies on lake level using satellite data (Table 1). For each of these water bodies, lake hypsometry was first constructed using time-varying water levels derived from ICESat and ICESat-2 and the corresponding water areas from Landsat images (Section 3.2). Water levels were retrieved by intersecting laser elevation measurements with dynamic water masks generated from the GSW water occurrence product (Section 3.2.2). The initial water area estimates at these water levels were delineated from Landsat images using multiple water indices (Section 3.2.1). To reduce errors in water area, the derived water levels were used to guide the refinements of initial water extents from Landsat images based on topographic

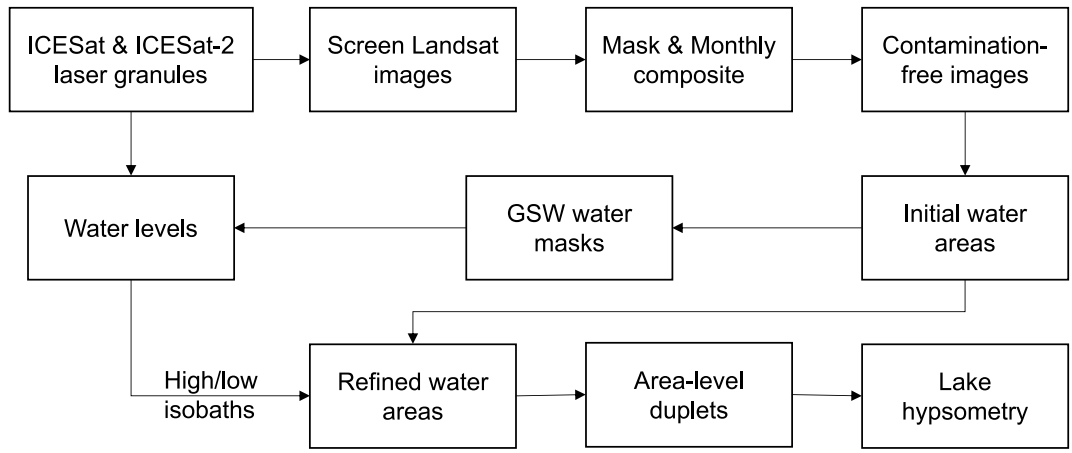

Figure 1. Schematic of construction of lake hypsometry from laser altimeters and Landsat images.

constraints (Section 3.2.3). The constructed lake hypsometry was combined with time-varying lake water areas in the GLATS data set to reconstruct multi-decadal lake levels (Section 3.3).

3.1. Studied Lakes

To test this proposed approach, we initially selected 400 lakes worldwide from the GLATS database as follows. We first screened lakes without reference level data and then randomly selected 400 water bodies among the remaining water bodies. Fifty-eight water bodies were further removed due to a lack of sufficient data for constructing lake hypsometry (see Section 3.2.4 for details). As a result, a total of 342 water bodies were finally selected for validation. These selected water bodies have various sizes (1–81,844 km^2), climate aridity (ranging from arid, to semi-arid, semi-humid, and humid), and elevation (1–4,911 m above sea level). They also include 294 large lakes (>50 km^2) and 48 small lakes (<50 km^2), which allows us to validate both large and small lakes across different climate regimes. Each selected water body has a multi-decadal water area record, as in the GLATS database, and observed water level data from in situ gauging stations (128 lakes) or radar altimetry (214 lakes) (Table 2).

3.2. Deriving Lake Hypsometry

To construct hypsometry, synchronous measurements of lake areas and water levels (i.e., area-level duplets) are required. We derived water levels from ICESat (2003–2009) and ICESat-2 (2018–2022) and the corresponding water areas from Landsat images (Figure 1). Given the relatively low temporal frequencies of Landsat (16 days) and laser altimetry satellites (91 days), monthly water areas and levels were used to generate area-level duplets, which is also in line with existing studies (Busker et al., 2019; Y. Li et al., 2020). Details are given below.

3.2.1. Calculating Initial Water Extents and Areas

We followed a recently developed water mapping algorithm (Yao et al., 2019) to delineate time-varying water extents to pair them with levels from ICESat and ICESat-2. For each lake, we first defined the region of interest (ROI) as a buffer region that contains a reference extent of this water body as depicted in the circa-2000 global lake inventory (Sheng et al., 2016). The ROI was up to triple the size of the reference extent to completely encompass the largest possible inundation extent during recent decades (2003–2022). We also ensured that the ROI excludes any major water bodies except the studied one. The ROI was used to filter the months with ICESat or ICESat-2 granules. All available Landsat images during these months were collected. These images were masked out of clouds, shadows, snow and ice, and mosaicked using a monthly median composite (see Yao et al. (2019) for details). The composited imagery increased the maximum coverage of good-quality observations in that month. If the good-quality portion was less than 95% of the ROI, the composited imagery was dropped. This filtering process balances the number and quality of images for constructing high-quality hypsometry (Y. Li et al., 2020).

Six commonly-used water indices, including the Normalized Difference Water Index (NDWI) (McFeeters, 1996), the Modified Normalized Difference Water Index (Xu, 2006), the High Resolution Water Index (Yao et al., 2015), the 2015 Water Index (WI2015) (Fisher et al., 2016), and two Automatic Water Extraction Indices (AWEInsh and AWEIsh) (Feyisa et al., 2014) (see Yao et al. (2019) for their configurations), were used to produce an ensemble of water area time series. Each water index was applied at the default threshold (here defined as zero) and the adaptive threshold, respectively, to generate two sets of water area time series per water index method. Considering the default threshold may not always yield accurate water delineation (J. Li & Sheng, 2012; J. Wang et al., 2014), the adaptive threshold was determined by Otsu's segmentation (Otsu, 1979) on the water index pixels within the ROI so that the adjusted threshold is likely to be more adaptive to the local conditions, such as aerosols and water quality. In total, each time step has 12 initial water extents and areas.

3.2.2. Estimating Water Levels

For each ICESat or ICESat-2 granule within the lake ROI, the laser elevation measurements were converted to the EGM2008 datum (Pavlis et al., 2012) to account for geoid variation. The geoid model of EGM2008 has an overall accuracy of about 0.2 m (Bergé-Nguyen et al., 2021). Converted elevations were grouped on a monthly basis to generate monthly water levels. As the ATL08 product provides elevation measurements of the terrestrial surface including both water and land, the 30-m GSW water occurrence map derived from 37-year Landsat observations (Pekel et al., 2016) was used to filter laser elevation points on the water surface. Unlike a recent study (Cooley et al., 2021) which generated a fixed water mask based on water occurrence, we used a dynamic water mask that best matches the actual water area for each month of the laser measurements. To do so, a total of 100 isobaths were generated from the GSW water occurrence map based on 100 distinct water occurrence values. The isobath with the closest area to the lower quartile of the initial water areas was selected as the water mask to filter laser elevation points on water. The lower quartile made the water area conservative, which ensured all laser elevation measurements on non-water surfaces, for example, due to classification errors, were screened (Cooley et al., 2021). The median elevation value of the filtered laser points was used as the water level for that month. To improve the accuracy, we dropped the water level in a month if less than six laser elevation points were available or the standard deviation of elevations from all laser points was higher than 1 m.

3.2.3. Refining Water Extents and Levels

The 12 sets of water extents as described in Section 3.2.1 were correlated with the water level data from ICESat/ICESat-2 and the set with the highest correlation was selected as the optimal set. However, remnant mapping errors could remain due to disturbances, such as cloud shadows and aquatic vegetation. To reduce these errors, we further refined the water extent based on topographic constraints, similar to Yao et al. (2019). The rationale was that the shoreline of a lake at a certain water level should be completely contained in any isobath with a higher level. Thus, we ranked the water extents based on the levels. We assumed that the errors caused by cloud shadows and seasonal vegetation were random, the two higher isobaths and two lower isobaths were used to reduce the commission and omission errors of the mapped water extent. The commission errors were identified as portions of "water" in the current extent that were beyond both higher isobaths. Similarly, if the water extent contained an "island" that was inundated by both two lower isobaths, the "island" was treated as an omission error and reclassified as water (Figure 2). The refined water areas were used to generate updated dynamic water masks using the GSW water occurrence map. We replaced the initial water areas with the refined water areas and followed the same steps in Section 3.2.2.

3.2.4. Constructing the Hypsometric Curve

The time-varying water areas and levels were paired by time to calibrate the hypsometric curve as a polynomial function (Crétaux et al., 2016) since area-level relationships can be non-linear (Figure 3b). We used the Akaike information criterion (AIC) to select the best polynomial model. AIC has a penalty term on the number of model parameters designed to minimize or avoid overfitting (Berk, 2008). However, a linear function was used in cases when there are less than 10 points (area-level duplets) for the fit or the fit polynomial function was not monotonic within the range of water areas or had a poor fit ($R^2 < 0.6$). We excluded a total of 58 (15%) lakes as they have less than three points (area-level duplets) for fitting a hypsometric curve. According to existing studies (Busker et al., 2019; Y. Li et al., 2020), if the hypsometry has a poor fit, the hypsometry should not be used due to high uncertainty. We found that only 49 (14%) lakes had a poor fit ($R^2 < 0.6$). Most of these lakes were affected by ice

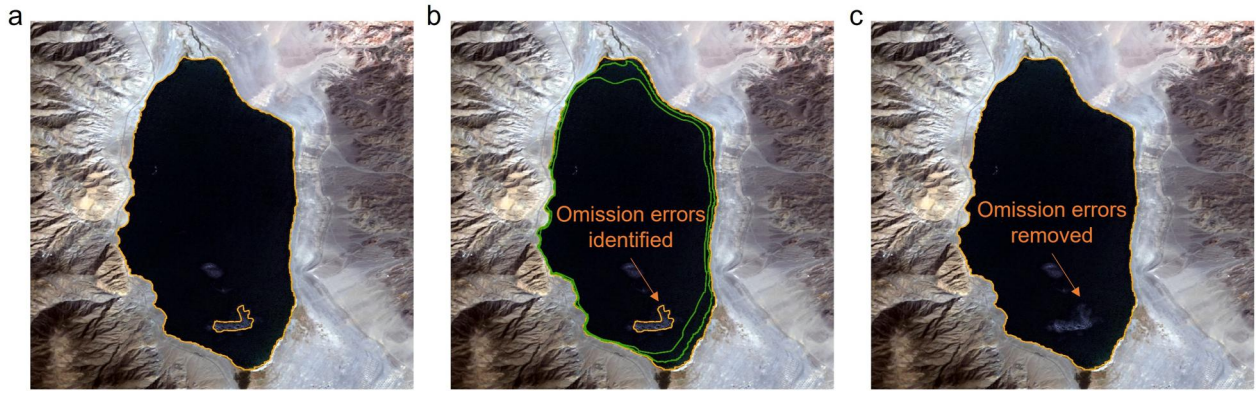

Figure 2. Illustration of removing omission errors using two lower isobaths using a case study of Walker Lake (38.70°N, 118.71°W) in Nevada (Figure adapted from Yao et al. (2019)). (a) Initial water extent (yellow line) in January 2007. (b) Identifying omission errors (e.g., island at the lake bottom) using two lower isobaths (green line). (c) Refined water extent (yellow) after removing the errors. Removing commission errors follows a similar concept except using two higher isobaths (Figure not shown).

cover, wetland vegetation communities, or exhibited small variations in water area, with a coefficient of variance less than 2%. We chose to keep these lakes as we preferred to report the overall accuracy of all lakes with sufficient data.

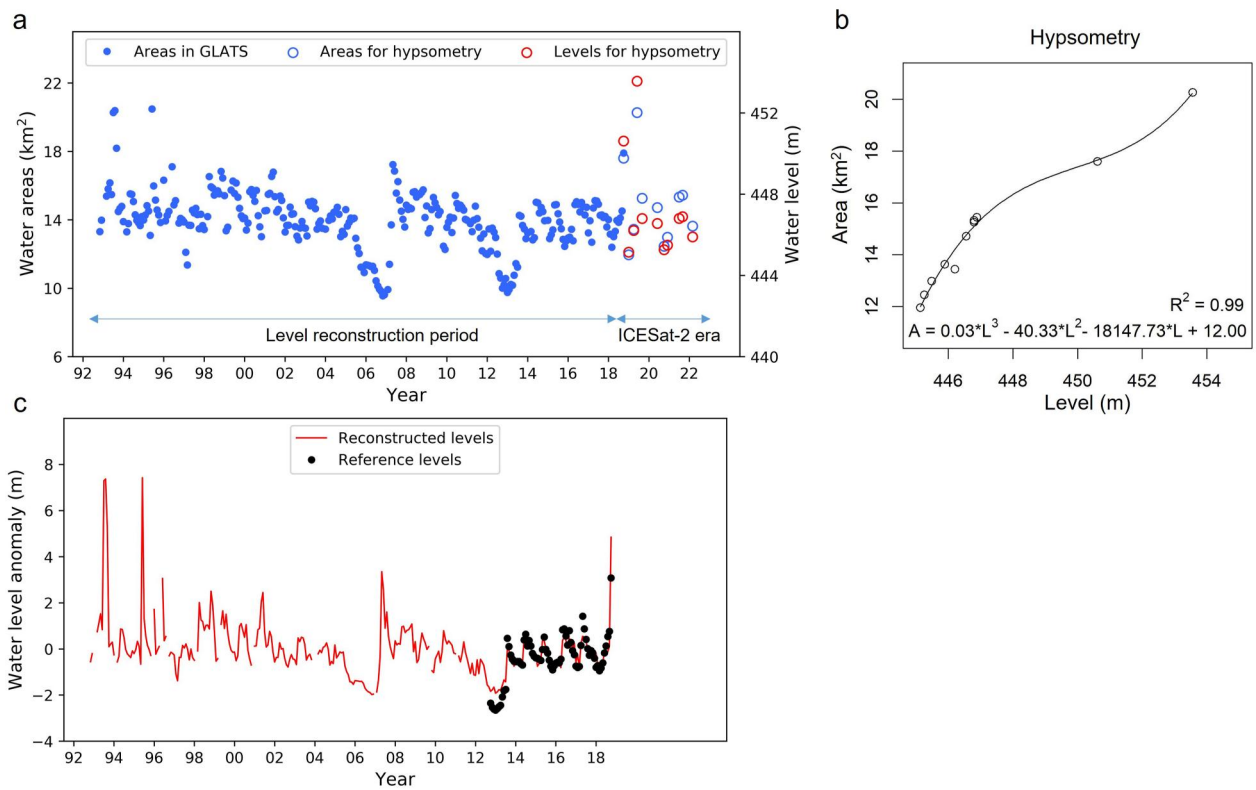

Figure 3. Illustration of level reconstruction using a case study of Lake Kanopolis (38.64°N, 98.01°W) in Kansas, USA. (a) Lake area time series during the level reconstruction period from Global Lake/Reservoir Area Time Series data set, as well as derived water levels from laser altimeters and mapped areas from Landsat for hypsometry construction. (b) Calibrated hypsometric curve (black line) using the stepwise polynomial fitting. (c) Reconstructed lake levels overlapped by reference levels from in situ measurements.

3.3. Reconstructing Multi-Decadal Water Levels

For each water body, hypsometry was used to convert water area time series from 1992 to 2018, as archived in the GLATS database (e.g., Figure 3a), to water levels. Lake level change was calculated through the hypsometric curve ($h = dA/dL$) over two consecutive water areas using the following equation:

$$\Delta L = h^{-1}(A_{t2}) - h^{-1}(A_{t1})$$

where ΔL denotes the water level change from an initial time ($t1$) with lake area (A_{t1}) to a later time ($t2$) with lake area (A_{t2}). We note that the hypsometric curve may need to be extrapolated to estimate some possible lower or higher water levels beyond the level range of the hypsometry (Busker et al., 2019; Schwatke et al., 2020; Weekley & Li, 2021; Yao et al., 2018). We calculated lake level changes for each time step relative to the initial time step, yielding a time series of relative lake levels (Figure 3c). Lake level anomalies were calculated from the relative lake levels by subtracting the long-term mean during the period (1992–2018).

3.4. Evaluating Reconstructed Water Level Products From In Situ Observations and Radar Altimeters

The reconstructed water levels were validated against observed water levels from in situ gauging stations or radar altimeters. The difference in overall accuracy between using in situ data and radar altimetry levels as reference sources appears to be minor based on the examination of the United States, where both data sets have good coverage (Figure S1). The referenced level data were aggregated into monthly medians, which were then used to validate the estimated water levels. To remove the impacts of different datums and altimetry tracks, water level anomalies were calculated for both estimated and referenced water levels over the overlapping period. The Root Mean Square Error (RMSE) was used to evaluate the accuracy of estimated water level anomalies. To assess the fidelity of the generated water level time series, RMSE normalized by the standard deviation of reference monthly levels (nRMSE) was also calculated. As existing studies indicated hypsometry is critical for scaling areas to levels (Crétaux et al., 2016), we assessed the impact of hypsometry on reconstructed levels, focusing on goodness of fit (R^2) of hypsometric curves and additional uncertainties caused by hypsometry extrapolation. Additionally, the accuracy of the trends and seasonal amplitude derived from reconstructed water levels was validated using the in situ data. The trend was calculated over the overlapping period using the Mann-Kendall method (Kendall, 1948). The lake level anomalies were deseasonalized before calculating the trend. The seasonal amplitude was calculated as the difference between maximum level and minimum level in a given year.

For comparison, we also validated the reconstructed water levels in two very recent studies (Y. Feng et al., 2022; Y. Li et al., 2023). The accuracy of our reconstructed water levels was compared separately with each of these two studies due to the difference in reconstructed water levels using altimetry-derived hypsometry. The comparison between this study and Y. Feng et al. (2022) involved 313 lakes that were included in both studies, while the comparison between this study and Y. Li et al. (2023) was limited to 82 lakes. Y. Li et al. (2023) constructed high-quality hypsometry ($R^2 > 0.5$) for 347 lakes using radar and ICESat altimeters and used empirical models to infer the hypsometry for the remaining 6,898 lakes archived in Global Reservoir and Dam database (GRandD, v1.3). We only compared with reconstructed water levels using altimetry-derived hypsometry in Y. Li et al. (2023).

4. Results

4.1. Accuracy of Reconstructed Lake Levels

The reconstructed lake levels agree with the water levels directly observed from radar altimeters, with a median RMSE value of 0.66 m (Figure 4a). For more than two-thirds of the studied water bodies, the reconstructed lake levels have sub-meter accuracy. We note that sub-meter accuracy is considered good for reconstructed levels that do not use direct observations from gauging stations or satellite altimetry (Zhan et al., 2021). Less than 15% of the studied water bodies have large errors (>2 m) (Figure 5a). Large RMSE values (>2 m) are mostly found in reservoirs and could be partially attributed to the difference in timing (e.g., a few days or weeks) between reconstructed levels and referenced levels that were compared on a monthly basis. Additionally, reconstructed lake level errors are mostly smaller than the standard deviation of monthly level variability (i.e., nRMSE <100%) (Figures 4b and 5b), providing useful information on both seasonal and inter-annual level variability. The median nRMSE is 57%. The overall performance between large and small water bodies is comparable in terms of both

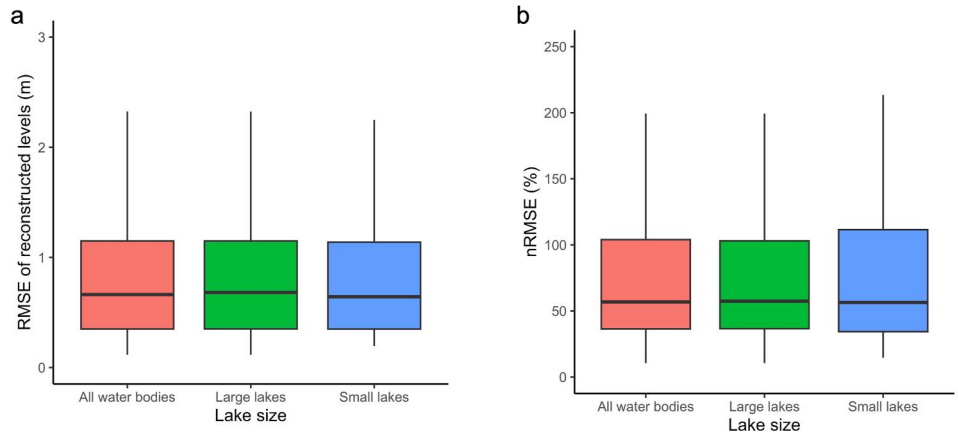

Figure 4. The uncertainty of reconstructed water levels for all water bodies, large lakes (>50 km^2), and small lakes (<50 km^2), validated against observed levels from in situ gauging stations or radar altimeters, expressed as (a) the Root Mean Square Error (RMSE) of the reconstructed water levels and (b) the normalized RMSE (nRMSE).

RMSE and nRMSE using the *t*-statistic ($p > 0.1$). For both large and small water bodies, the RMSE of reconstructed levels is smaller than the standard deviation of level variability for over 70% of studied water bodies.

To facilitate potential applications of the proposed method, we also report the accuracy of the trend and seasonal amplitude derived from reconstructed levels by validating them against the reference data during the overlapping period. The estimated trending rates generally align well with the values obtained from the reference data, as indicated by the R^2 value of 0.92 and slope of 0.94 (Figure 6a). The RMSE of the estimated trends is 0.10 m yr^{-1}. However, concerning seasonal variations, the seasonal amplitude appears to be underestimated with a slope of 0.84 and an RMSE of 3.01 m (Figure 6b). These discrepancies in seasonal amplitude can be attributed to factors such as insufficient temporal coverage and poorly fit hypsometry. For example, excluding 148 (43%) water bodies with a poorly fit hypsometry ($R^2 < 0.6$) or temporal frequency less than bi-monthly (mostly in cold regions), the RMSE reduces from 3.01 to 2.18 m and the R^2 increases from 0.65 to 0.85 (Figure 6c). Additionally, the underestimation is largely alleviated as indicated by an updated slope of 0.94. Thus, the remaining reconstructed levels (57%) can provide reliable information on seasonal amplitude.

4.2. Impact of Hypsometry on Water Level Reconstruction

The hypsometry needs to be extrapolated to estimate lower or higher water levels beyond the level range of the hypsometry. The median proportion of extrapolated levels is 29% for all studied lakes and slightly higher for small water bodies (32%) owing to infrequent overlapping laser altimetry tracks over smaller water extents (Cooley et al., 2021). For all water bodies, adding the extrapolated water levels increases the temporal frequency by a median of one-third but leads to a moderate increase of the median RMSE from 0.59 to 0.66 m or normalized RMSE from 53% to 57%, compared with the errors of interpolated water levels (Figures 7a and 7d). The median RMSE and nRMSE values for all extrapolated levels are 0.78 m and 72%, respectively. For both large and small water bodies, the RMSE and nRMSE of extrapolated levels are larger than those of interpolated levels (Figures 7b, 7c, 7e, and 7f). Thus, we confirm that the hypsometry extrapolation increases uncertainty in reconstructing water levels as reported previously (e.g., Crétaux et al., 2016), which should be considered when analyzing the level time series.

The median R^2 of the constructed hypsometry is 0.92 for all water bodies. Small lakes have a slightly higher R^2 with a median of 0.94 (Figure 8a). For a majority of both large and small lakes (>85%), the R^2 of the constructed hypsometry is greater than 0.6. Only 14% of lakes have a poor hypsometry ($R^2 < 0.6$). However, errors (RMSE and nRMSE) of reconstructed levels from poorly fit hypsometry exhibit a much larger spread (Figures 8b and 8c). Roughly 45% of reconstructed levels with a poorly fit hypsometry have either a RMSE value larger than 2 m or a nRMSE value larger than 200%. These indicate reconstructed levels from poorly fit hypsometry need to be interpreted with care if they are used at all. Most of the poorly fit hypsometry are found in lakes with small relative area variations (<5%), such as the Great Lakes of North America.

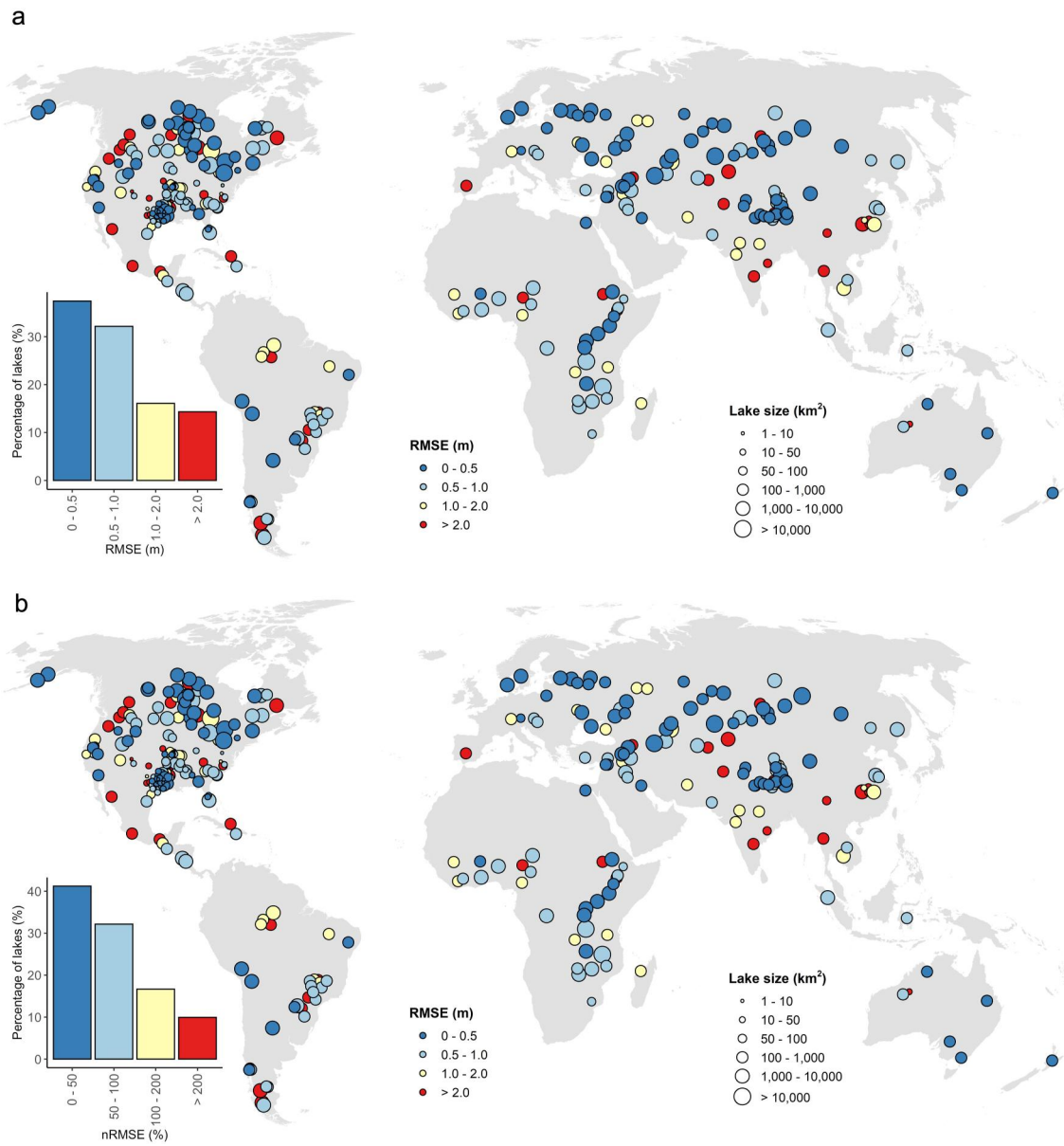

Figure 5. Spatial portrayal of uncertainties in reconstructed water levels, expressed as the (a) RMSE and (b) nRMSE, with respective histograms shown in the insets.

To evaluate the relative performance of our reconstructed levels, we compared our reconstructed levels with existing reconstructed level data from altimetry-derived hypsometry as in Y. Feng et al. (2022) and Y. Li et al. (2023). Evaluated on 313 overlapping lakes, the median RMSE of Y. Feng et al. (2022) is 0.77 m, with an interquartile range (IQR) of 0.84 m. The median RMSE of this study is 0.56 m, which is 0.21 m (27%) more accurate than Y. Feng et al. (2022), and the interquartile range is less spread by 0.22 m (26%) (Figure 9a). This improvement could be explained by the fact that the hypsometry of this study exhibits much stronger area-level correlations than that of Y. Feng et al. (2022). For example, the median R^2 increased from 0.43 to 0.93 (Figure 9b). Compared with Y. Li et al. (2023) on 82 lakes, the median RMSE of this study is 0.39 m (32%) more accurate than Y. Li et al. (2023) (Figure 9c). This improvement was likely owing to the incorporation of the more accurate levels from ICESat-2 and refining water areas (Figure 9d) as most of the high-quality hypsometry in Y. Li et al. (2023) was constructed using ICESat and GSW data set.

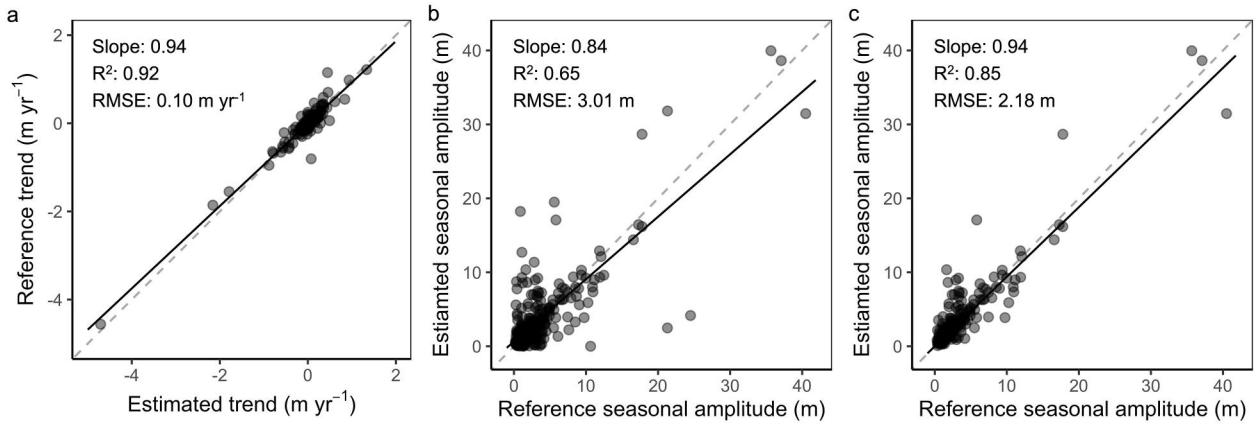

Figure 6. The uncertainty of the water level trends and seasonal amplitude derived from reconstructed levels. (a) Trends for all 342 water bodies. (b) Seasonal amplitude for all 342 water bodies. (c) Seasonal amplitude for 192 water bodies with a good hypsometry ($R^2 > 0.6$) and temporal frequency equal to or higher than bi-monthly.

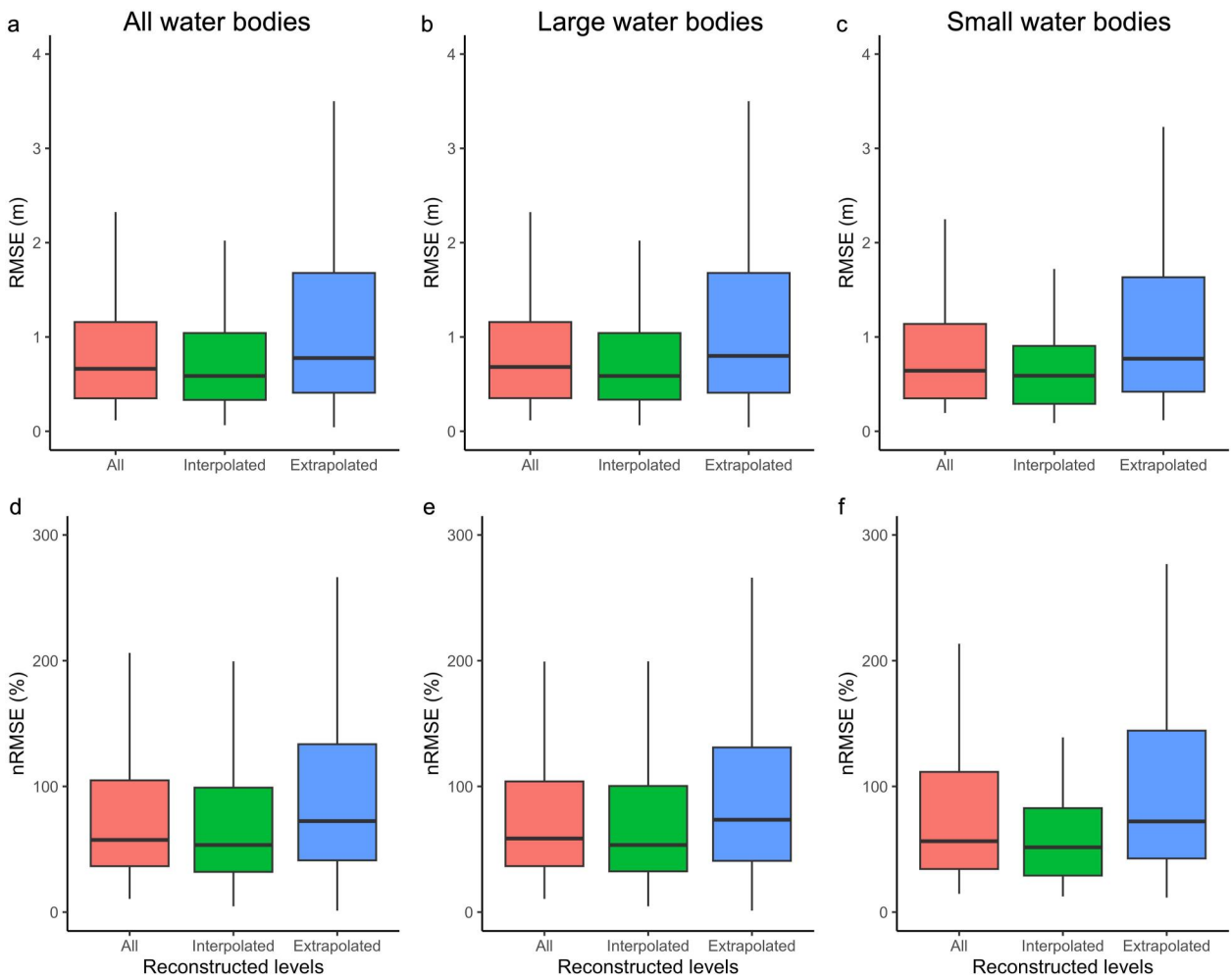

Figure 7. The impact of hypsometry extrapolation on the accuracy of the reconstructed levels, expressed by the Root Mean Square Error (RMSE) for all reconstructed levels, interpolated levels, and extrapolated levels, and similarly for the nRMSE. (a) RMSE and (d) nRMSE for all water bodies. (b) RMSE and (e) nRMSE for large water bodies. (c) RMSE and (f) nRMSE for small water bodies.

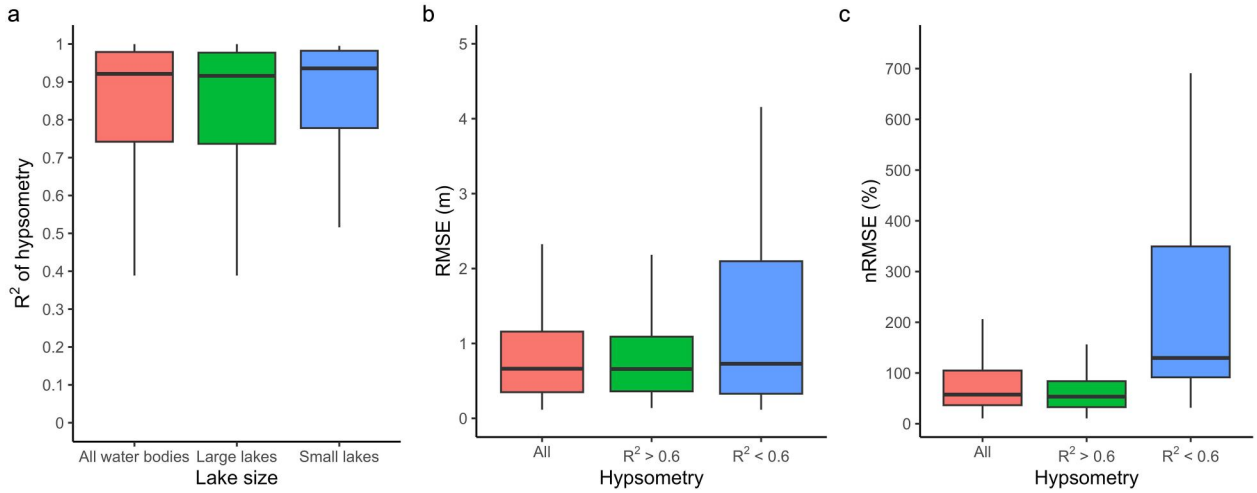

Figure 8. The uncertainties of reconstructed levels from high-quality ($R^2 > 0.6$) and poorly-fitted ($R^2 < 0.6$) hypsometry. (a) R^2 of constructed hypsometry for all water bodies, large lakes, and small lakes. (b) RMSE. (c) nRMSE.

4.3. Time Series of Reconstructed Lake Water Levels

Reconstructed lake water levels show strong agreement with reference levels in terms of both seasonal and decadal variability (Figure 10). For instance, estimated water level in Lake Maraboon in Australia showed a decline by 5.0 m over the period 1993–1996 and then increased by 6.5 m between 1996 and 1999. These estimated changes are relatively close to the reference level variations from in situ observations of 5.4 and 7.5 m, respectively (Figure 10a). Our time series also captures differences in seasonal variability from year to year (Figures 10b and 10d) and level extremes (Figure 10c). In some cases, reconstructed water levels are more temporally consistent than the reference levels, since the latter suffer from missing data caused by the disfunction of in situ gauging stations or mission gaps of radar altimeters (Figure 10a). While the reference levels from radar altimeters in different databases are overall consistent, some discrepancies exist due to different data sources and processing methods (Figures 10e and 10f). For example, the RMSE of reconstructed levels for Lake Mar Chiquita in Argentina against the Hydroweb levels is 0.27 m, whereas the RMSE values are 0.34 and 0.86 m, respectively, when validating against the G-RLEAM and the DAHITI levels (Figure 10f). Thus, the uncertainty in reference levels from radar altimeters may impact our reported accuracy, although the impact was minimized by reporting

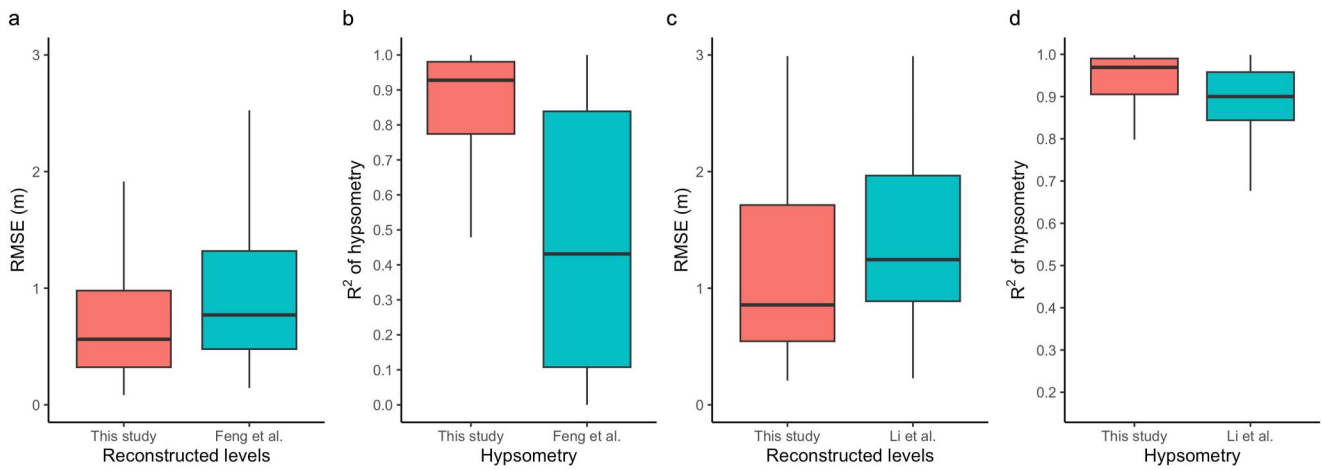

Figure 9. Comparison of the accuracy of reconstructed levels between this study and existing studies. (a) Root Mean Square Error (RMSE) of reconstructed levels between this study and Y. Feng et al. (2022). (b) R^2 of hypsometry between this study and Y. Feng et al. (2022). (c) RMSE of reconstructed levels between this study and Y. Li et al. (2023). (d) R^2 of hypsometry between this study and Y. Li et al. (2023). Comparison between this study and Y. Feng et al. (2022) involved 313 lakes, while 82 lakes were included in the comparison between this study and Y. Li et al. (2023).

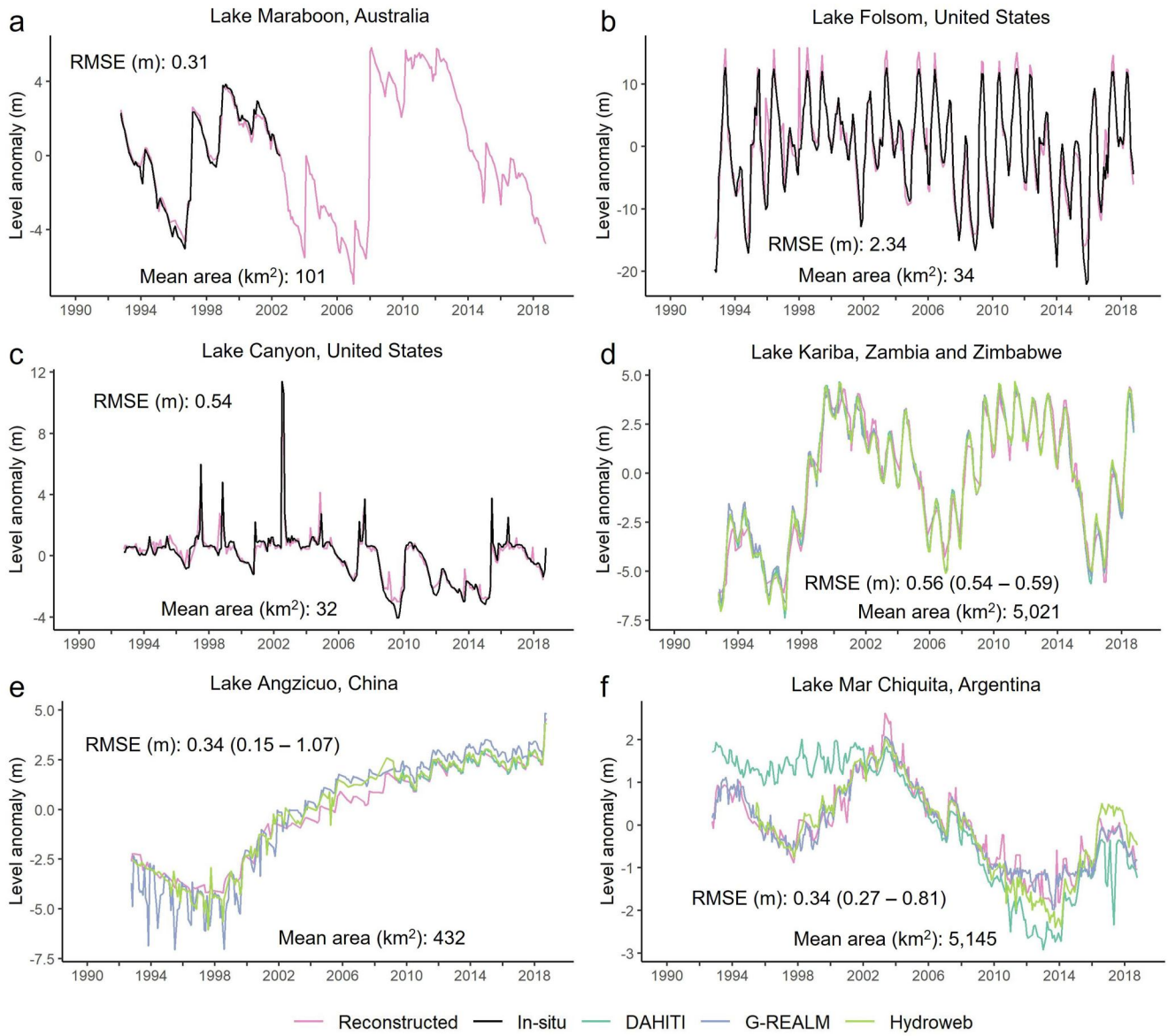

Figure 10. Reconstructed water levels and reference levels for Lake Maraboon (147.97°E, 23.70°S) in Australia, Lakes Folsom (98.20°W, 29.90°N) and Canyon (121.13°W, 38.70°N) in the United States, Lake Kariba (27.93°E, −17.01°S) on the border of Zambia and Zimbabwe, Lake Angzicuo (87.15°E, 31.03°N) in China, and Lake Mar Chiquita (−62.70°W, 30.59°S) in Argentina. The Root Mean Square Error (RMSE) shown in each panel is the RMSE of reconstructed levels against observed levels from in situ gauges or radar altimeters. When validating against different level products from radar altimeters, the median of the RMSE values was reported first, followed by the lowest RMSE and the highest RMSE in brackets.

the median of the RMSE values against all available level products, for example, 0.34 m for Lake Mar Chiquita. If we assume that the "true" error is between the lowest error and highest error of validations against different reference levels, the median RMSE of all reconstructed lake levels is in the range of (0.64 m, 0.71 m). This narrow range is around the reported RMSE (0.66 m), indicating the uncertainty in reference levels likely has a negligible impact on our reported accuracy.

The reconstructed water levels mostly achieve a temporal frequency greater than bi-monthly, during the 1992–2018 study period (Figure 11). For water bodies in the tropical and sub-tropical regions where most of the global population (>60%) resides, reconstructed levels cover every two out of three monthly steps on average. However, relatively low temporal frequencies, for example, less than four times per year, are mostly found in water bodies at high-latitude (>45°N) or high-altitude regions (e.g., Tibetan Plateau) (Figure 11) because of a

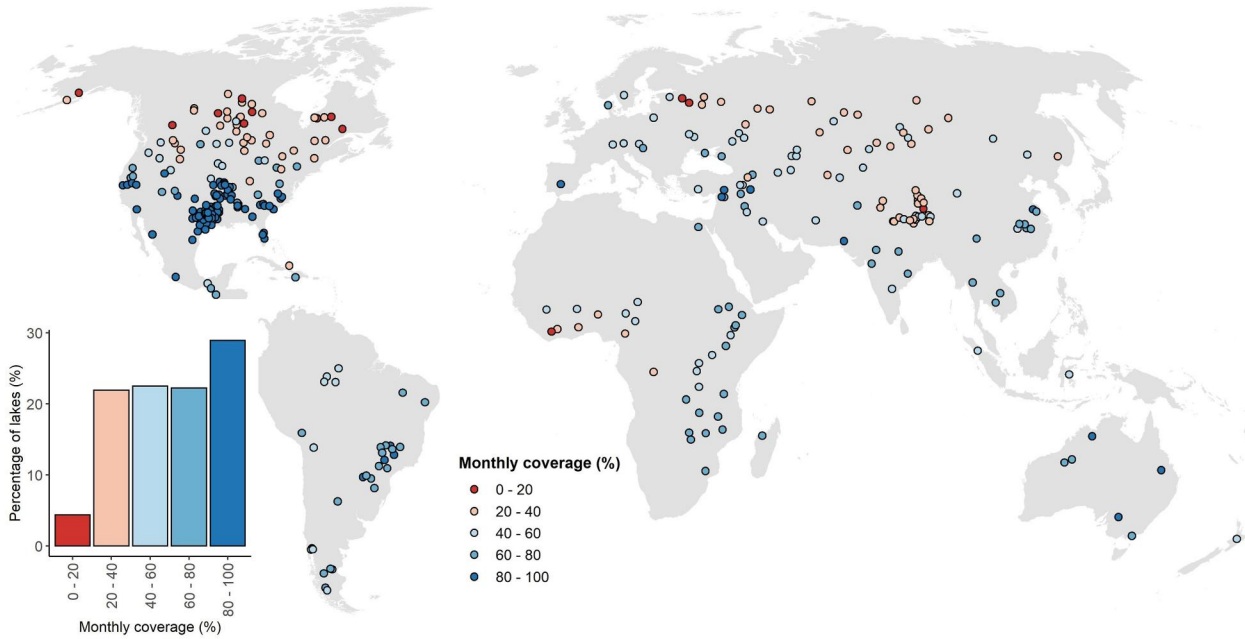

Figure 11. Monthly coverage of reconstructed water levels (1992–2018). The inset shows the histogram.

prolonged freezing season when water bodies are covered by snow and ice and their extents and boundaries cannot easily be detected from satellite images (Yao et al., 2019). Nevertheless, cold-region lakes typically exhibit notable level changes during ice-free seasons (Crétaux et al., 2016) for which our method is applicable. For example, reconstructed levels for two-thirds of studied lakes on the Tibetan Plateau cover over half of the monthly steps during ice-free seasons. Therefore, resulting water levels from our method can also provide insights into level variability and driving hydrological processes in poorly monitored cold regions.

5. Discussion

Despite the importance of lake level monitoring, global in situ data that are publicly accessible are in decline (Schwatke et al., 2015). Existing inland water level data sets from satellites are limited by spatial coverage (Birkett et al., 2011; Crétaux et al., 2011; Schwatke et al., 2015), short records (Cooley et al., 2021), or large gaps in their time series (Luo et al., 2022). To overcome these limitations, our approach leveraged the extended spatial coverage of high-resolution laser altimeters and the long duration of fine-resolution Landsat images to construct time-varying lake levels spanning multiple decades without a major gap. Validated on 342 water bodies with sizes ranging from 1 to 81,844 km^2, our reconstructed multi-decadal water levels show sub-meter accuracy for roughly two-thirds of the studied water bodies. We consider the sub-meter accuracy of water levels to be good, considering that this is a proxy-based approach without direct observations from satellite altimeters (Zhan et al., 2021). The reported accuracy here is comparable to the accuracy of water levels estimated from Landsat imagery and in situ bathymetry (Weekley & Li, 2019). Thus, our method provides a promising alternative to reconstructing multi-decadal water levels of both large and small water bodies that have not been consistently monitored for decades.

The accuracy of reconstructed water levels from a proxy-based approach like this study depends on the data quality of both lake areas and hypsometry. Recent advances in water area mapping from satellites largely ameliorated the trade-off between spatial and temporal resolutions in mapping time-varying water areas by recovering water areas from contaminated images, for example, those affected by clouds or observation gaps (Schwatke et al., 2019; Yao et al., 2019; Zhao & Gao, 2018). The GLATS data set used in this study has a reported error of only 2.2% in recovered areas from contaminated Landsat images (Yao et al., 2019). The improved water area time series can be combined with hypsometry data to reconstruct water levels at a near-monthly resolution spanning more than 30 years. However, high-quality lake hypsometry data are limited to a few hundred of lakes due to low area-level correlations (Crétaux et al., 2016; Y. Li et al., 2023; Yao et al., 2023). As poorly fit

hypsometry may introduce large uncertainties (e.g., Figures 8b and 8c), existing studies either screened out a large number of altimetry-observed water bodies with poorly fit hypsometry (Busker et al., 2019; Y. Li et al., 2020), or relied on simplified hypsometry to estimate levels with large uncertainties (Y. Feng et al., 2022; Yao et al., 2023). Compared with recently reconstructed lake level data (Y. Feng et al., 2022), we increased the median R^2 of the hypsometry from 0.43 to 0.92 (Figure 9b). The hypsometry for more than 85% of studied water bodies here achieves a good fit ($R^2 > 0.6$), indicating our approach is more robust than existing methods.

Other factors affecting the accuracy of reconstructed levels include the availability of ICESat data and the bathymetry changes due to sedimentation. The footprint size of ICESat-2 (∼17-m) is finer than that of ICESat (∼70-m), thus some lakes may only have data from ICESat-2. Excluding ICESat data, the median RMSE and nRMSE of reconstructed water levels are 0.74 m and 64%, which are slightly larger than the reported values (0.66 m and 57%). Sediment-induced bathymetry change in natural lakes should not be a significant factor at interannual to decadal scales given notable sedimentation-induced bathymetry changes occur over very long timescales (e.g., over one thousand years) (Singh et al., 1972). Sedimentation rates in reservoirs are larger partially due to reduced outflow (Lee & Foster, 2013). The mean annual reservoir sedimentation rate is reported to be 0.5%–1% of full storage (Basson, 2009). For most reservoirs, the uncertainty of estimated water level changes due to sedimentation should be no larger than 0.1%, 1%, and 10% at monthly, yearly, and decadal scales, respectively, if we assume a similar relative error in water level from sedimentation. For reservoirs with severe sedimentation (e.g., due to high sediment load from rivers and landslides), the results may need to be interpreted with care.

The approach presented here can be used to estimate long-term level trends and intra-annual level variability, as well as to assess climate change impacts on lake levels, for a water body individually or a group of water bodies over a large domain. In particular, water levels at the basin scale are highly relevant to water resource management (Pascolini-Campbell et al., 2020). These scales are often sparsely monitored, or not monitored at all (Crétaux et al., 2011). This approach can help fill this gap by producing higher-frequency multi-decadal water levels for both large and small water bodies. Particularly, levels in small water bodies were often unmonitored despite their local importance on water supply and outsized roles on surface water extent variability (Pi et al., 2022) and carbon cycling (Holgerson & Raymond, 2016). As shown in Figure 11, the temporal frequency of reconstructed levels is mostly higher than bi-monthly over the past 26 years in tropical and sub-tropical basins where most of the global population (>60%) resides. Additionally, errors in reconstructed levels were typically lower than the standard derivation of level variability during the reconstruction period, thus providing useful information on seasonal and inter-annual level changes. This approach can be used to monitor the impact of climate extremes on lake levels, which is becoming increasingly important. For example, the largest freshwater body Lake Poyang in China went from nearly dry to the highest level on record during 2019–2020 (Wei et al., 2020), while nearly all large lakes in East Africa reached extremely high levels by the end of 2019, never seen over the last 20 years (Papa et al., 2022). By contrast, the largest US reservoir Lake Mead reached its lowest level in August 2021, triggering the first-ever federal declaration of water shortages (Hung et al., 2022). Another interesting application of this method is to derive lake bathymetry in combination with climate reconstructions for reconstructing paleolake levels (Gill et al., 2015) which play a key part in understanding the past hydroclimate and potentially projecting future variability.

The improved reconstruction of water levels here also provides new opportunities to expand and update existing estimates on lake water storage, particularly given that lake level is often the most crucial variable that determines water storage variability (Cooley et al., 2021). Despite recent advances on documenting long-term changes in lake water storage (Y. Feng et al., 2022; Y. Li et al., 2023; Luo et al., 2022; Yao et al., 2023), water storage data are unavailable for most small water bodies and poorly constrained for some large lakes due to simplified hypsometries or empirical models (Table 1). The level reconstruction method here can be combined with lake area data sets (Pi et al., 2022; Yao et al., 2019; Zhao & Gao, 2018) to fill this data gap. Furthermore, the improvements in water storage estimates can be useful for constraining the uncertainties associated with attributing water storage changes to natural and anthropogenic factors, which are often debated (Rodell et al., 2018; Wurtsbaugh et al., 2017; Yao et al., 2023).

We further anticipate this method will become increasingly useful in particular as more data become available from ICESat-2 and the more recent Surface Water and Ocean Topography (SWOT) mission (launched in December 2022). SWOT will provide unprecedented measurements of both water areas and water levels for all lakes larger than 0.01 km^2 at a 21-day cycle, owing to wide-swath Interferometric Synthetic Aperture Radar

(InSAR) techniques (Biancamaria et al., 2016). New level measurements from SWOT and ICESat-2 would improve relative ranges and goodness of fit (R^2) of hypsometric curves, leading to more accurate level reconstructions. Given that ICESat-2 and SWOT can observe hundreds of thousands of water bodies or more, the method presented here may be applicable to monitor a large majority of these water bodies and thus inform water resource management to a much greater extent than is achieved currently.

6. Conclusions

In this study, we developed a novel and transferrable approach to reconstruct high-frequency multi-decadal water levels of natural lakes and reservoirs across the globe by leveraging the extended spatial coverage of high-resolution laser altimeters and the long duration of fine-resolution Landsat images. Evaluation of 342 water bodies worldwide demonstrated that most reconstructed lake levels have sub-meter accuracy with a median RMSE of 0.66 m. Despite the short records of ICESat and ICESat-2 observations, the temporal frequency of reconstructed lake levels is mostly higher than bi-monthly during the past 26 years, owing to utilizing a proxy-based approach to scale water areas into levels. The constructed hypsometry exhibited strong correlations between water areas and levels with an R^2 value greater than 0.6 for over 85% of studied water bodies, suggesting this method is more robust than existing methods for deriving high-quality lake hypsometry and long-term water levels.

More broadly, this study provides important guidance for studying long-term water level and volume variability using limited data from existing and future satellite missions. Particularly, we demonstrate that water levels can be reconstructed beyond the short lifetime of satellite altimeters when combined with longer duration missions (e.g., Landsat series). Owing to its generalizable nature, the presented method can be easily adapted to other InSAR and lidar sensors, such as SWOT. Despite a 3-year planned lifetime of SWOT, this method can leverage short-term level measurements via SWOT and enhance the capability of SWOT on long-term water level and volume studies.

Data Availability Statement

The Landsat images used in this manuscript were accessed from the Google Earth Engine platform at https://earthengine.google.com. ICESat and ICESat-2 data were downloaded from the National Snow and Ice Data Center at https://nsidc.org/data. Global Lake/Reservoir Area Time Series data set was obtained from Yao et al. (2019), which is accessible at https://lakewatch.users.earthengine.app/view/glats. The GSW data set was downloaded at https://global-surface-water.appspot.com/. In situ water levels were obtained from the USGS National Water Information System at https://waterdata.usgs.gov/nwis/, the U.S. Army Corps at https://water.usace.army.mil/ and https://nicholasinstitute.duke.edu/reservoir-data/, the Texas Water Development Board at https://waterdatafortexas.org/reservoirs/statewide/, the International Date Centre on Hydrology of Lakes and Reservoirs (HYDROLARE) at http://hydrolare.net/, the Canadian Water Office at https://wateroffice.ec.gc.ca/, and the Bureau of Meteorology in Australia can be downloaded from http://www.bom.gov.au/waterdata/. Water level products from radar altimeters were downloaded from the Hydroweb at http://hydroweb.theia-land.fr, the Database for Hydrological Time Series of Inland Waters (DAHITI) at https://dahiti.dgfi.tum.de/en, and the USDA G-REALM database at https://ipad.fas.usda.gov/cropexplorer/global_reservoir. The existing lake hypsometry from ICESat and radar altimeters were downloaded from https://dataverse.tdl.org/dataset.xhtml?persistentId=doi:10.18738/T8/TO5HJG. The reconstructed water levels and lake hypsometry, as well as data used for validation, are available on the zenodo data repository at https://doi.org/10.5281/zenodo.8190809.

Acknowledgments
This research was supported by the CIRES Visiting Fellows Program, funded by the NOAA Cooperative Agreement NA17OAR4320101, the CIRES Innovative Research Program, and the EI Climate Fellows Program to F. Yao. We thank the computing support from the Alpine supercomputer, which is supported by the National Science Foundation (awards ACI-1532235 and ACI-1532236), the University of Colorado Boulder, and Colorado State University. We thank Tim Smith and Michael Diamond for proofreading this manuscript.

References

Abdalati, W., Zwally, H. J., Bindschadler, R., Csatho, B., Farrell, S. L., Fricker, H. A., et al. (2010). The ICESat-2 laser altimetry mission. *Proceedings of the IEEE*, *98*(5), 735–751. https://doi.org/10.1109/JPROC.2009.2034765

Allen, G. H., & Pavelsky, T. M. (2018). Global extent of rivers and streams. *Science*, *361*(6402), 585–588. https://doi.org/10.1126/science.aat0636

Alsdorf, D. E., Rodriguez, E., & Lettenmaier, D. P. (2007). Measuring surface water from space. *Reviews of Geophysics*, *45*(2), RG2002. https://doi.org/10.1029/2006RG000197

Al-Weshah, R. A. (2000). The water balance of the Dead Sea: An integrated approach. *Hydrological Processes*, *14*(1), 145–154. https://doi.org/10.1002/(SICI)1099-1085(200001)14:1<145::AID-HYP916>3.0.CO;2-N

Barnett, T. P., & Pierce, D. W. (2008). When will Lake Mead go dry? *Water Resources Research*, *44*(3), W03201. https://doi.org/10.1029/2007WR006704

Basson, G. R. (2009). Management of siltation in existing and new reservoirs. In *General Report Q. 89. Proceedings of the 23rd Congress of the International Commission on Large Dams CIGBICOLD* (Vol. 2).

Bastviken, D., Tranvik, L. J., Downing, J. A., Crill, P. M., & Enrich-Prast, A. (2011). Freshwater methane emissions offset the continental carbon sink. *Science*, *331*(6013), 50. https://doi.org/10.1126/science.1196808

Bergé-Nguyen, M., Cretaux, J.-F., Calmant, S., Fleury, S., Satylkanov, R., Chontoev, D., & Bonnefond, P. (2021). Mapping mean lake surface from satellite altimetry and GPS kinematic surveys. *Advances in Space Research*, *67*(3), 985–1001. https://doi.org/10.1016/j.asr.2020.11.001

Berk, R. A. (2008). *Statistical learning from a regression perspective* (Vol. 14). Springer. https://doi.org/10.1007/978-0-387-77501-2_1

Biancamaria, S., Lettenmaier, D. P., & Pavelsky, T. M. (2016). The SWOT mission and its capabilities for land hydrology. *Surveys in Geophysics*, *37*(2), 307–337. https://doi.org/10.1007/s10712-015-9346-y

Birkett, C., Reynolds, C., Beckley, B., & Doorn, B. (2011). From Research to Operations: The USDA Global Reservoir and Lake Monitor. In *Coastal altimetry* (pp. 19–50). Springer Berlin Heidelberg. https://doi.org/10.1007/978-3-642-12796-0_2

Bootsma, H. A., & Hecky, R. E. (1993). Conservation of the African Great Lakes: A limnological perspective. *Conservation Biology*, *7*(3), 644–656. https://doi.org/10.1046/j.1523-1739.1993.07030644.x

Busker, T., de Roo, A., Gelati, E., Schwatke, C., Adamovic, M., Bisselink, B., et al. (2019). A global lake and reservoir volume analysis using a surface water dataset and satellite altimetry. *Hydrology and Earth System Sciences*, *23*(2), 669–690. https://doi.org/10.5194/hess-23-669-2019

Chaudhari, S., Felfelani, F., Shin, S., & Pokhrel, Y. (2018). Climate and anthropogenic contributions to the desiccation of the second largest saline lake in the twentieth century. *Journal of Hydrology*, *560*, 342–353. https://doi.org/10.1016/j.jhydrol.2018.03.034

Chen, J. L., Pekker, T., Wilson, C. R., Tapley, B. D., Kostianoy, A. G., Cretaux, J., & Safarov, E. S. (2017). Long-term Caspian Sea level change. *Geophysical Research Letters*, *44*(13), 6993–7001. https://doi.org/10.1002/2017GL073958

Cooley, S. W., Ryan, J. C., & Smith, L. C. (2021). Human alteration of global surface water storage variability. *Nature*, *591*(7848), 78–81. https://doi.org/10.1038/s41586-021-03262-3

Crétaux, J.-F., Abarca-del-Río, R., Bergé-Nguyen, M., Arsen, A., Drolon, V., Clos, G., & Maisongrande, P. (2016). Lake volume monitoring from space. *Surveys in Geophysics*, *37*(2), 269–305. https://doi.org/10.1007/s10712-016-9362-6

Crétaux, J.-F., Jelinski, W., Calmant, S., Kouraev, A., Vuglinski, V., Bergé-Nguyen, M., et al. (2011). SOLS: A lake database to monitor in the near real time water level and storage variations from remote sensing data. *Advances in Space Research*, *47*(9), 1497–1507. https://doi.org/10.1016/j.asr.2011.01.004

Crétaux, J.-F., Letolle, R., & Bergé-Nguyen, M. (2013). History of Aral Sea level variability and current scientific debates. *Global and Planetary Change*, *110*, 99–113. https://doi.org/10.1016/j.gloplacha.2013.05.006

Dawadi, S., & Ahmad, S. (2012). Changing climatic conditions in the Colorado River Basin: Implications for water resources management. *Journal of Hydrology*, *430*, 127–141. https://doi.org/10.1016/j.jhydrol.2012.02.010

Donchyts, G., Baart, F., Winsemius, H., Gorelick, N., Kwadijk, J., & van de Giesen, N. (2016). Earth's surface water change over the past 30 years. *Nature Climate Change*, *6*(9), 810–813. https://doi.org/10.1038/nclimate3111

Feng, L., Pi, X., Luo, Q., & Li, W. (2023). Reconstruction of long-term high-resolution lake variability: Algorithm improvement and applications in China. *Remote Sensing of Environment*, *297*, 113775. https://doi.org/10.1016/j.rse.2023.113775

Feng, Y., Zhang, H., Tao, S., Ao, Z., Song, C., Chave, J., et al. (2022). Decadal lake volume changes (2003–2020) and driving forces at a global scale. *Remote Sensing*, *14*(4), 1032. https://doi.org/10.3390/rs14041032

Feyisa, G. L., Meilby, H., Fensholt, R., & Proud, S. R. (2014). Automated Water Extraction Index: A new technique for surface water mapping using Landsat imagery. *Remote Sensing of Environment*, *140*, 23–35. https://doi.org/10.1016/j.rse.2013.08.029

Fisher, A., Flood, N., & Danaher, T. (2016). Comparing Landsat water index methods for automated water classification in eastern Australia. *Remote Sensing of Environment*, *175*, 167–182. https://doi.org/10.1016/j.rse.2015.12.055

Gao, H., Birkett, C., & Lettenmaier, D. P. (2012). Global monitoring of large reservoir storage from satellite remote sensing. *Water Resources Research*, *48*(9), 2012WR012063. https://doi.org/10.1029/2012WR012063

Gill, E. C., Rajagopalan, B., & Molnar, P. H. (2015). An assessment of the mean annual precipitation needed to sustain Lake Sambhar in Rajasthan, India, during mid-Holocene time. *The Holocene*, *25*(12), 1923–1934. https://doi.org/10.1177/0959683615596817

Gorelick, N., Hancher, M., Dixon, M., Ilyushchenko, S., Thau, D., & Moore, R. (2017). Google Earth Engine: Planetary-scale geospatial analysis for everyone. *Remote Sensing of Environment*, *202*, 18–27. https://doi.org/10.1016/j.rse.2017.06.031

Gronewold, A. D., & Stow, C. A. (2014). Water loss from the Great Lakes. *Science*, *343*(6175), 1084–1085. https://doi.org/10.1126/science.1249978

Hipsey, M. R., Bruce, L. C., Boon, C., Busch, B., Carey, C. C., Hamilton, D. P., et al. (2019). A General Lake Model (GLM 3.0) for linking with high-frequency sensor data from the Global Lake Ecological Observatory Network (GLEON). *Geoscientific Model Development*, *12*(1), 473–523. https://doi.org/10.5194/gmd-12-473-2019

Holgerson, M. A., & Raymond, P. A. (2016). Large contribution to inland water CO_2 and CH_4 emissions from very small ponds. *Nature Geoscience*, *9*(3), 222–226. https://doi.org/10.1038/ngeo2654

Hung, F., Son, K., & Yang, Y. C. E. (2022). Investigating uncertainties in human adaptation and their impacts on water scarcity in the Colorado River Basin, United States. *Journal of Hydrology*, *612*, 128015. https://doi.org/10.1016/j.jhydrol.2022.128015

Kendall, M. G. (1948). Rank correlation methods.

Khandelwal, A., Karpatne, A., Ravirathinam, P., Ghosh, R., Wei, Z., Dugan, H. A., et al. (2022). ReaLSAT, a global dataset of reservoir and lake surface area variations. *Scientific Data*, *9*(1), 1–12. https://doi.org/10.1038/s41597-022-01449-5

Lee, C., & Foster, G. (2013). Assessing the potential of reservoir outflow management to reduce sedimentation using continuous turbidity monitoring and reservoir modelling. *Hydrological Processes*, *27*(10), 1426–1439. https://doi.org/10.1002/hyp.9284

Li, J., & Sheng, Y. (2012). An automated scheme for glacial lake dynamics mapping using Landsat imagery and digital elevation models: A case study in the Himalayas. *International Journal of Remote Sensing*, *33*(16), 5194–5213. https://doi.org/10.1080/01431161.2012.657370

Li, X., Long, D., Huang, Q., Han, P., Zhao, F., & Wada, Y. (2019). High-temporal-resolution water level and storage change data sets for lakes on the Tibetan Plateau during 2000–2017 using multiple altimetric missions and Landsat-derived lake shoreline positions. *Earth System Science Data*, *11*(4), 1603–1627. https://doi.org/10.5194/essd-11-1603-2019

Li, Y., Gao, H., Zhao, G., & Tseng, K. H. (2020). A high-resolution bathymetry dataset for global reservoirs using multi-source satellite imagery and altimetry. *Remote Sensing of Environment*, *244*, 111831. https://doi.org/10.1016/j.rse.2020.111831

Li, Y., Zhao, G., Allen, G. H., & Gao, H. (2023). Diminishing storage returns of reservoir construction. *Nature Communications*, *14*(1), 3203. https://doi.org/10.1038/s41467-023-38843-5

Luo, S., Song, C., Ke, L., Zhan, P., Fan, C., Liu, K., et al. (2022). Satellite laser altimetry reveals a net water mass gain in global lakes with spatial heterogeneity in the early 21st century. *Geophysical Research Letters*, *49*(3), e2021GL096676. https://doi.org/10.1029/2021GL096676

Ma, S., Liao, J., Jing, R., & Chen, J. (2024). A dataset of lake level changes in China between 2002 and 2023 using multi-altimeter data. *Big Earth Data*, 1–23. https://doi.org/10.1080/20964471.2023.2295632

Madson, A., & Sheng, Y. (2021). Automated water level monitoring at the continental scale from ICESat-2 photons. *Remote Sensing*, *13*(18), 3631. https://doi.org/10.3390/rs13183631

Markus, T., Neumann, T., Martino, A., Abdalati, W., Brunt, K., Csatho, B., et al. (2017). The Ice, Cloud, and land Elevation Satellite-2 (ICESat-2): Science requirements, concept, and implementation. *Remote Sensing of Environment*, *190*, 260–273. https://doi.org/10.1016/j.rse.2016.12.029

McFeeters, S. K. (1996). The use of the Normalized Difference Water Index (NDWI) in the delineation of open water features. *International Journal of Remote Sensing*, *17*(7), 1425–1432. https://doi.org/10.1080/01431169608948714

McIntyre, P. B., Liermann, C. A. R., & Revenga, C. (2016). Linking freshwater fishery management to global food security and biodiversity conservation. *Proceedings of the National Academy of Sciences of the United States of America*, *113*(45), 12880–12885. https://doi.org/10.1073/pnas.1521540113

Micklin, P. P. (1988). Desiccation of the Aral Sea: A water management disaster in the Soviet Union. *Science*, *241*(4870), 1170–1176. https://doi.org/10.1126/science.241.4870.1170

Otsu, N. (1979). A threshold selection method from gray-level histograms. *IEEE Transactions on Systems, Man, and Cybernetics*, *9*(1), 62–66. https://doi.org/10.1109/TSMC.1979.4310076

Papa, F., Crétaux, J.-F., Grippa, M., Robert, E., Trigg, M., Tshimanga, R. M., et al. (2022). Water resources in Africa under global change: Monitoring surface waters from space. *Surveys in Geophysics*, *44*, 1–51. https://doi.org/10.1007/s10712-022-09700-9

Pascolini-Campbell, M. A., Reager, J. T., & Fisher, J. B. (2020). GRACE-based mass conservation as a validation target for basin-scale evapotranspiration in the contiguous United States. *Water Resources Research*, *56*(2), e2019WR026594. https://doi.org/10.1029/2019WR026594

Pavlis, N. K., Holmes, S. A., Kenyon, S. C., & Factor, J. K. (2012). The development and evaluation of the Earth Gravitational Model 2008 (EGM2008). *Journal of Geophysical Research*, *117*(B4), B04406. https://doi.org/10.1029/2011JB008916

Pekel, J.-F., Cottam, A., Gorelick, N., & Belward, A. S. (2016). High-resolution mapping of global surface water and its long-term changes. *Nature*, *540*(7633), 418–422. https://doi.org/10.1038/nature20584

Pi, X., Luo, Q., Feng, L., Xu, Y., Tang, J., Liang, X., et al. (2022). Mapping global lake dynamics reveals the emerging roles of small lakes. *Nature Communications*, *13*(1), 5777. https://doi.org/10.1038/s41467-022-33239-3

Rodell, M., Famiglietti, J. S., Wiese, D. N., Reager, J. T., Beaudoing, H. K., Landerer, F. W., & Lo, M. H. (2018). Emerging trends in global freshwater availability. *Nature*, *557*(7707), 651–659. https://doi.org/10.1038/s41586-018-0123-1

Rosenberg, D. E. (2022). Adapt Lake Mead releases to inflow to give managers more flexibility to slow reservoir drawdown. *Journal of Water Resources Planning and Management*, *148*(10), 02522006. https://doi.org/10.1061/(ASCE)WR.1943-5452.0001592

Ryan, J. C., Smith, L. C., Cooley, S. W., Pitcher, L. H., & Pavelsky, T. M. (2020). Global characterization of inland water reservoirs using ICESat-2 altimetry and climate reanalysis. *Geophysical Research Letters*, *47*(17), e2020GL088543. https://doi.org/10.1029/2020GL088543

Schutz, B. E., Zwally, H. J., Shuman, C. A., Hancock, D., & DiMarzio, J. P. (2005). Overview of the ICESat mission. *Geophysical Research Letters*, *32*(21), L21S01. https://doi.org/10.1029/2005GL024009

Schwatke, C., Dettmering, D., Bosch, W., & Seitz, F. (2015). DAHITI – An innovative approach for estimating water level time series over inland waters using multi-mission satellite altimetry. *Hydrology and Earth System Sciences*, *19*(10), 4345–4364. https://doi.org/10.5194/hess-19-4345-2015

Schwatke, C., Dettmering, D., & Seitz, F. (2020). Volume variations of small inland water bodies from a combination of satellite altimetry and optical imagery. *Remote Sensing*, *12*(10), 1606. https://doi.org/10.3390/rs12101606

Schwatke, C., Scherer, D., & Dettmering, D. (2019). Automated extraction of consistent time-variable water surfaces of lakes and reservoirs based on Landsat and Sentinel-2. *Remote Sensing*, *11*(9), 1010. https://doi.org/10.3390/rs11091010

Sheng, Y., Song, C., Wang, J., Lyons, E. A., Knox, B. R., Cox, J. S., & Gao, F. (2016). Representative lake water extent mapping at continental scales using multi-temporal Landsat-8 imagery. *Remote Sensing of Environment*, *185*, 129–141. https://doi.org/10.1016/j.rse.2015.12.041

Shugar, D. H., Burr, A., Haritashya, U. K., Kargel, J. S., Watson, C. S., Kennedy, M. C., et al. (2020). Rapid worldwide growth of glacial lakes since 1990. *Nature Climate Change*, *10*(10), 939–945. https://doi.org/10.1038/s41558-020-0855-4

Singh, G., Joshi, R. D., & Singh, A. B. (1972). Stratigraphic and radiocarbon evidence for the age and development of three salt lake deposits in Rajasthan, India. *Quaternary Research*, *2*(4), 496–505. https://doi.org/10.1016/0033-5894(72)90088-9

Tao, S., Fang, J., Zhao, X., Zhao, S., Shen, H., Hu, H., et al. (2015). Rapid loss of lakes on the Mongolian Plateau. *Proceedings of the National Academy of Sciences*, *112*(7), 2281–2286. https://doi.org/10.1073/pnas.1411748112

Tilzer, M. M., & Serruya, C. (1990). In M. M. Tilzer & C. Serruya (Eds.), *Large lakes*. Springer Berlin Heidelberg. https://doi.org/10.1007/978-3-642-84077-7

Tokuda, D., Kim, H., Yamazaki, D., & Oki, T. (2021). Development of a coupled simulation framework representing the lake and river continuum of mass and energy (TCHOIR v1.0). *Geoscientific Model Development*, *14*(9), 5669–5693. https://doi.org/10.5194/gmd-14-5669-2021

Wang, J., Sheng, Y., Gleason, C. J., & Wada, Y. (2013). Downstream Yangtze River levels impacted by Three Gorges Dam. *Environmental Research Letters*, *8*(4), 044012. https://doi.org/10.1088/1748-9326/8/4/044012

Wang, J., Sheng, Y., & Tong, T. S. D. (2014). Monitoring decadal lake dynamics across the Yangtze Basin downstream of Three Gorges Dam. *Remote Sensing of Environment*, *152*, 251–269. https://doi.org/10.1016/j.rse.2014.06.004

Wang, J., Sheng, Y., & Wada, Y. (2017). Little impact of the Three Gorges Dam on recent decadal lake decline across China's Yangtze Plain. *Water Resources Research*, *53*(5), 3854–3877. https://doi.org/10.1002/2016WR019817

Wang, J., Song, C., Reager, J. T., Yao, F., Famiglietti, J. S., Sheng, Y., et al. (2018). Recent global decline in endorheic basin water storages. *Nature Geoscience*, *11*(12), 926–932. https://doi.org/10.1038/s41561-018-0265-7

Wang, Y., Long, D., & Li, X. (2023). High-temporal-resolution monitoring of reservoir water storage of the Lancang-Mekong River. *Remote Sensing of Environment*, *292*, 113575. https://doi.org/10.1016/j.rse.2023.113575

Weekley, D., & Li, X. (2019). Tracking multidecadal lake water dynamics with Landsat imagery and topography/bathymetry. *Water Resources Research*, *55*(11), 8350–8367. https://doi.org/10.1029/2019WR025500

Weekley, D., & Li, X. (2021). Tracking lake surface elevations with proportional hypsometric relationships, Landsat imagery, and multiple DEMs. *Water Resources Research*, *57*(1), e2020WR027666. https://doi.org/10.1029/2020WR027666

Wei, K., Ouyang, C., Duan, H., Li, Y., Chen, M., Ma, J., et al. (2020). Reflections on the catastrophic 2020 Yangtze River Basin flooding in southern China. *The Innovation*, *1*(2), 100038. https://doi.org/10.1016/j.xinn.2020.100038

Williamson, C. E., Saros, J. E., Vincent, W. F., & Smol, J. P. (2009). Lakes and reservoirs as sentinels, integrators, and regulators of climate change. *Limnology and Oceanography*, *54*(6part2), 2273–2282. https://doi.org/10.4319/lo.2009.54.6_part_2.2273

Wurtsbaugh, W. A., Miller, C., Null, S. E., DeRose, R. J., Wilcock, P., Hahnenberger, M., et al. (2017). Decline of the world's saline lakes. *Nature Geoscience*, *10*(11), 816–821. https://doi.org/10.1038/ngeo3052

Wurtsbaugh, W. A., & Sima, S. (2022). Contrasting management and fates of two sister lakes: Great Salt Lake (USA) and Lake Urmia (Iran). *Water*, *14*(19), 3005. https://doi.org/10.3390/w14193005

Xu, H. (2006). Modification of normalised difference water index (NDWI) to enhance open water features in remotely sensed imagery. *International Journal of Remote Sensing*, *27*(14), 3025–3033. https://doi.org/10.1080/01431160600589179

Yao, F., Livneh, B., Rajagopalan, B., Wang, J., Crétaux, J.-F., Wada, Y., & Berge-Nguyen, M. (2023). Satellites reveal widespread decline in global lake water storage. *Science*, *380*(6646), 743–749. https://doi.org/10.1126/science.abo2812

Yao, F., Wang, C., Dong, D., Luo, J., Shen, Z., & Yang, K. (2015). High-resolution mapping of urban surface water using ZY-3 multi-spectral imagery. *Remote Sensing*, *7*(9), 12336–12355. https://doi.org/10.3390/rs70912336

Yao, F., Wang, J., Wang, C., & Crétaux, J.-F. (2019). Constructing long-term high-frequency time series of global lake and reservoir areas using Landsat imagery. *Remote Sensing of Environment*, *232*, 111210. https://doi.org/10.1016/j.rse.2019.111210

Yao, F., Wang, J., Yang, K., Wang, C., Walter, B. A., & Crétaux, J.-F. (2018). Lake storage variation on the endorheic Tibetan Plateau and its attribution to climate change since the new millennium. *Environmental Research Letters*, *13*(6), 064011. https://doi.org/10.1088/1748-9326/aab5d3

Yuan, C., Gong, P., & Bai, Y. (2020). Performance assessment of ICESat-2 laser altimeter data for water-level measurement over lakes and reservoirs in China. *Remote Sensing*, *12*(5), 770. https://doi.org/10.3390/rs12050770

Zhan, P., Song, C., Luo, S., Liu, K., Ke, L., & Chen, T. (2021). Lake level reconstructed from DEM-based virtual station: Comparison of multisource DEMs with laser altimetry and UAV-LiDAR measurements. *IEEE Geoscience and Remote Sensing Letters*, *19*, 1–5. https://doi.org/10.1109/LGRS.2021.3086582

Zhang, G., Xie, H., Kang, S., Yi, D., & Ackley, S. F. (2011). Monitoring lake level changes on the Tibetan Plateau using ICESat altimetry data (2003–2009). *Remote Sensing of Environment*, *115*(7), 1733–1742. https://doi.org/10.1016/j.rse.2011.03.005

Zhao, G., & Gao, H. (2018). Automatic correction of contaminated images for assessment of reservoir surface area dynamics. *Geophysical Research Letters*, *45*(12), 6092–6099. https://doi.org/10.1029/2018GL078343